Experimental observation of phase-flip transitions in the brain

Nicholas M. Dotson and Charles M. Gray
Cell Biology and Neuroscience, Montana State University, Bozeman, Montana 59717, USA
(Received 6 May 2016; revised manuscript received 14 September 2016; published 24 October 2016)

The phase-flip transition has been demonstrated in a host of coupled nonlinear oscillator models, many pertaining directly to understanding neural dynamics. However, there is little evidence that this phenomenon occurs in the brain. Using simultaneous microelectrode recordings in the nonhuman primate cerebral cortex, we demonstrate the presence of phase-flip transitions between oscillatory narrow-band local field potential signals separated by several centimeters. Specifically, we show that sharp transitions between in-phase and antiphase synchronization are accompanied by a jump in synchronization frequency. These findings are significant for two reasons. First, they validate predictions made by model systems. Second, they have potentially far reaching implications for our understanding of the mechanisms underlying corticocortical communication, which are thought to rely on narrow-band oscillatory synchronization with specific relative phase relationships.

DOI: 10.1103/PhysRevE.94.042420

I. INTRODUCTION

Coupled nonlinear oscillator systems with time delay have been heavily studied due to the inherent time delays in real world systems, including the nervous system [1–4]. A salient feature of time-delay coupled systems is the phase-flip transition, which is defined by a flip between 0° (in phase) and 180° (antiphase) in the relative phase with a concurrent jump in synchronization frequency [5]. Indeed, analytical investigations of time-delay coupled limit cycle oscillators, Rössler oscillators, excitable laser models, predator prey models, Nishio-Inaba circuits, and several neuronal spiking models have all reported flips between 0° and 180° in the relative phase as a function of time delay, typically with a concurrent jump in synchronization frequency [5–8]. Experimentally, the phase-flip transition has been demonstrated in a living coupled oscillator system of the plasmodium of the slime mold and coupled electrochemical cells [9,10]. More complex coupling schemes between nonlinear oscillators, such as indirect coupling [11,12] and coupling with asymmetrical delays [13], have demonstrated the phase-flip transition as well. Interestingly, asymmetrical coupling leads to phase relationships that deviate from 0° and 180°. This body of work indicates that the phase-flip transition is a characteristic property of time-delay coupled systems, and common to systems with nontrivial coupling schemes as well.

Although many studies of time-delay coupled systems pertaining directly or indirectly to understanding neural dynamics have reported phase-flip transitions, there is little experimental evidence documenting this phenomenon in the brain. In a previous publication, we demonstrated that oscillatory narrow-band local field potential signals within and between prefrontal and posterior parietal cortex tend to synchronize near 0° and near 180° during a visual working memory task, indicating that the relative phase relationship may provide a means for segregating neuronal networks [14]. Immediately following the end of the working memory task, we observed abrupt transitions between the dominant phase relationships (∼0° and ∼180°), in a subset of signal pairs, analogous to a phase-flip transition. However, we did not determine if there was a concurrent jump in synchronization frequency, which is a distinguishing property of the phase-flip transition. In this paper, we use a different data set, with different areal combinations, to demonstrate that the phase-flip transition between oscillatory narrow-band local field potential signals involves both a phase flip and a jump in synchronization frequency. We then discuss the potential function of this phenomenon within the context of corticocortical communication.

II. METHODS

A. Experimental setup

A macaque monkey was implanted with a large-scale microelectrode recording device capable of making simultaneous recordings—both action potentials and local field potentials—from 256 microelectrodes distributed across an entire hemisphere (see Ref. [15] for more details). All procedures were performed in accordance with NIH guidelines and the Institutional Animal Care and Use Committee of Montana State University. Broadband neuronal activity was recorded on each viable electrode while the monkey performed an oculomotor, delayed match-to-sample task that involved remembering a centrally presented sample image for ∼1 s (similar to the task used in Refs. [14,16]). Here we analyze the data from correct trials during the period immediately after the task, referred to as the intertrial interval (ITI). The duration of the ITI is ∼1.6 s. The ITI begins immediately after the match-to-sample trial is over and ends at the start of the next match-to-sample trial. At this point in time a small fluid reward is given and the animal is free to look around the room. This study focuses on the ITI for two reasons. First, the ITI is the period of time when large changes in the relative phase relationships were previously observed [14]. Second, the ITI begins immediately after a cognitively demanding task and is followed by a short period of time when the animal may rest. Changes in activity during the ITI may reflect changes in neuronal sate.

In this paper we use data from somatosensory areas 1, 2, and 3, frontal area 5, and prefrontal areas 8L and 9/46d, collected across 13 recording sessions. Figure 1(a) shows an example of the recording sites from a single recording session superimposed on a schematic of the nonhuman primate brain (channels 1–7). Since electrodes penetrate the cortex, the

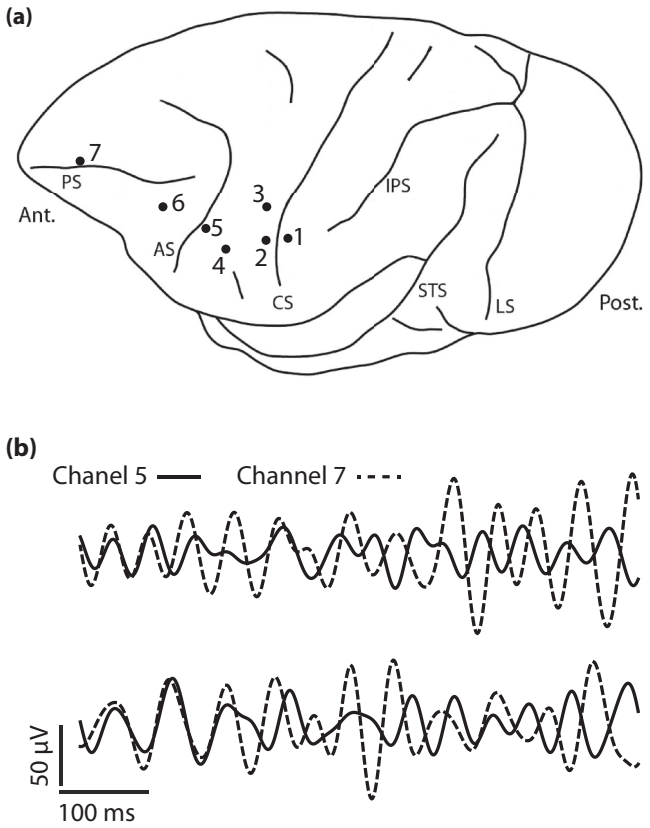

FIG. 1. Schematic of the nonhuman primate brain and example data. (a) The brain is shown from anterior (Ant.) to posterior (Post.), with sulci labeled for reference. (PS) Principal sulcus. (AS) Arcuate sulcus. (CS) Central sulcus. (IPS) Intraparietal sulcus. (STS) Superior temporal sulcus. (LS) Lunate sulcus. (b) Bandpassed (8–25 Hz) local field potential signals for two trials during the ITI. The signals are from channel 5 (solid line) and channel 7 (dashed line). Time and voltage scales are provided at the bottom left of the plot.

location of each recording site is approximate. The recordings in Fig. 1(a) are from somatosensory area 2 (channel 1), somatosensory area 1 (channel 2), somatosensory area 3 (channel 3), frontal area 5 (channels 4 and 5), prefrontal area 8L (channel 6), and prefrontal area 9/46d (channel 7). During each recording session, subsets of electrodes were moved. These cortical areas were selected for this analysis based on a preliminary screen for signal pairs with both changes in their relative phase relationships and sufficiently strong correlations (typically >0.1) in the frequency range of interest. Many combinations of cortical areas in the full data set do not show phase flips during the ITI. Indeed, only certain combinations of areas in the selected data show phase flips. A full description of the dynamics of all signal pairs is beyond the scope of this paper.

B. Analysis methods

To estimate the average relative phase relationship and synchronization frequency over time for each pair of signals, we use a sliding window cross-correlation analysis. First, the data is bandpass filtered between 8 and 25 Hz using a zero phase forward and reverse digital infinite impulse response (IIR) fourth-order Butterworth filter and then downsampled to 1 kHz. The bandpass parameters are motivated by preliminary results showing phase locking within this band (data not shown) and our previous study [14]. Figure 1(b) shows the bandpassed data for channel 5 and channel 7 on two example trials, both of which show a clear transition from in-phase to antiphase synchronization. Next, we calculate the average normalized cross-correlogram (200 ms windows; 50 ms step; ± 100 ms lag; for more details, see Ref. [14]) using all correct trials ($n = 274$). Finally, the relative phase angle and synchronization frequency are estimated by fitting an eight-parameter generalized Gabor function (GF) to each cross-correlogram [14,17],

$$\mathrm{GF}(t) = Ae^{-\left(\frac{|t-\Delta t|}{\sigma_1}\right)^{\lambda}} \cos[2\pi f(t-\Delta t)] + O + Be^{\left(-\frac{t}{\sigma_2}\right)^2}, \quad (1)$$

where A is the amplitude of the function, Δt is the time lag, σ_1 is a decay constant, λ is an exponent ($\lambda = 2$ for the standard Gabor function), f is the frequency, O is the offset, B is the central modulation factor ($B = 0$ for the standard Gabor function), and σ_2 is the width of the central peak. Each GF is fit using the Levenberg-Marquardt algorithm in *Matlab*. The synchronization frequency is simply f and we calculate the relative phase angle (ϕ) in degrees by using f and the time lag (Δt) as follows: $\phi = 360^\circ f\,\Delta t$. This provides us with a single value for both the relative phase angle and the synchronization frequency during each time step for each combination of signal pairs.

III. EXPERIMENTAL RESULTS

Using the sliding window analysis we were able to determine the time course of the relative phase and synchronization frequency during the ITI for each pair of signals. Figure 2(a) shows an example of the sliding window analysis for channels 5 (frontal area 5) and 7 (prefrontal area 9/46d) from the example recording session used in Fig. 1. In this example, we clearly see that the relative phase flips from near in phase to near antiphase. During the early part of the ITI the relative phase is near 0° and the peak correlation coefficient is near 0.15. At around 350–400 ms the correlation drops close to 0, which may be due to these time windows overlapping the period when the signals are transitioning from in phase to antiphase. Following this period of desynchronization, the signals are near antiphase and the strength of correlation goes back up (in this case they are negatively correlated so the sign is negative). We note that a correlation coefficient around $|0.15|$ is similar to previous observations of long-range correlations [14]. In Fig. 2(b) we show both the relative phase and the synchronization frequency over time for the example in Fig. 2(a). We see that the frequency jumps from $\sim$12 to $\sim$18 Hz when the relative phase flips from near in phase to near antiphase, demonstrating a typical phase-flip transition.

The relative phase values over time for all signal pairs from the example recording session (Fig. 1) are shown in Fig. 3. Here we see that the relative phase of many of the signal pairs changes very little, while others show a phase flip. Not all of the phase flips are as clean as the results in the Fig. 2 example, and some may not be considered a full

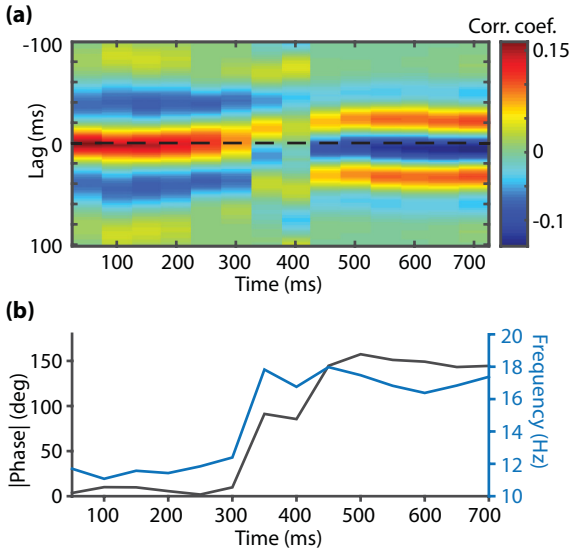

FIG. 2. Example phase-flip transition between channel 5 and channel 7. (a) Gabor functions (fit to each average cross-correlogram) at each time step (x axis), with time lag on the y axis and the correlation coefficient shown in color on the z axis. (b) Relative phase (left y axis) and synchronization frequency (right y axis) over time.

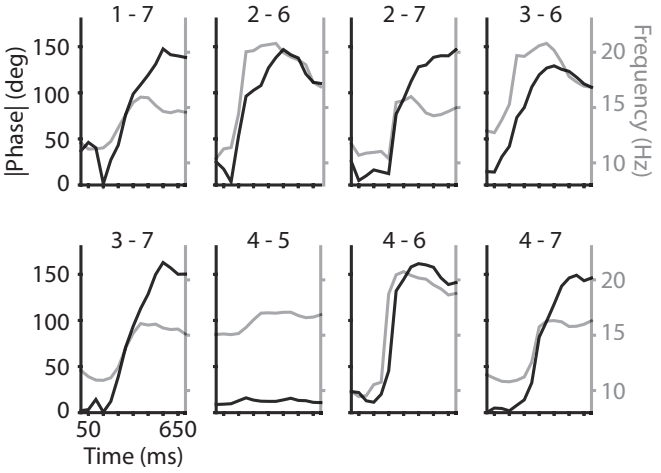

FIG. 4. Summary of the relative phase and synchronization frequency for six example signal pairs. The relative phase (dark gray; absolute value) is on the left y axis. The synchronization frequency (light gray) is on the right y axis. Channel numbers are indicated at the top of each figure. Signals are from somatosensory area 2 (channel 1), somatosensory area 1 (channel 2), somatosensory area 3 (channel 3), frontal area 5 (channels 4 and 5), prefrontal area 8L (channel 6), and prefrontal area 9/46d (channel 7).

phase flip. However, the signal pairs including prefrontal area 8L (channel 6) or prefrontal area 9/46d (channel 7) typically undergo a phase flip during the middle of the ITI. Figure 4 highlights several of these phase flips, showing the same relative phase data presented in Fig. 3 (channel combinations in bold font) and the associated synchronization frequency.

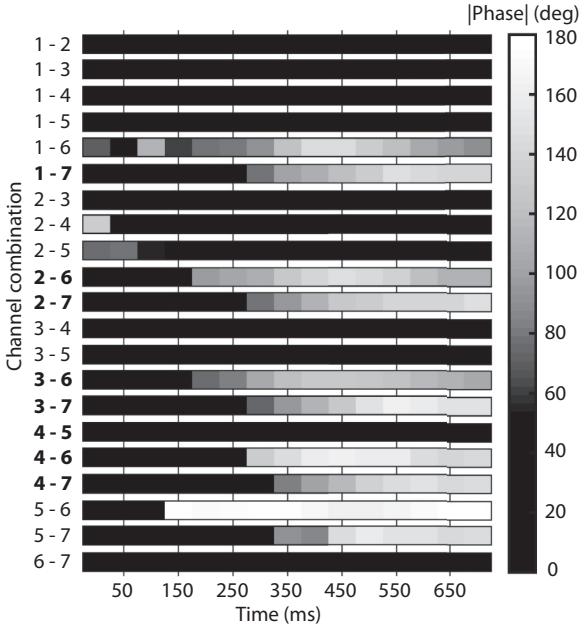

FIG. 3. Summary of the relative phase over time, for all signal pairs from example session. Each horizontal bar shows the relative phase for a single signal pair. Gray scale indicates the relative phase, from in phase (black) to antiphase (white).

Similar to the example shown in Fig. 2, the signal pairs with a flip in their relative phase have a concurrent jump in their synchronization frequency. We show the data for channel 4 and channel 5 to demonstrate that small changes in the relative phase and frequency still occur on signal pairs that do not undergo a phase-flip transition. There is also a substantial amount of variability in both the changes in relative phase and synchronization frequency. For example, the synchronization frequency between channel 4 and channel 6 nearly doubles between the early and late ITI, while the change in synchronization frequency between channel 1 and channel 7 is only a few Hz.

Using data from 13 recording sessions—including the example session used in the previous figures—we verify that phase-flip transitions consistently occur between prefrontal area 9/46d or prefrontal area 8L and the somatosensory areas (1, 2, and 3) and frontal area 5. Data were pooled in order to have enough data points to test for differences in the relative phase angles and synchronization frequencies. This resulted in a total of 12 signal pairs with area 9/46d and somatosensory areas 1 (two signal pairs), 2 (four signal pairs), and 3 (two signal pairs), and frontal area 5 (four signal pairs); and a total of 26 signal pairs with area 8L and somatosensory areas 1 (three signal pairs), 2 (13 signal pairs), and 3 (five signal pairs), and frontal area 5 (five signal pairs). We used the frequency and relative phase data during the early part of the ITI (50 ms after ITI start) and the late part of the ITI (700 ms after ITI start) for each pair of signals to determine if phase-flip transitions occurred across the population. Figure 5(a) shows the distribution of frequencies for all combinations of signals from somatosensory areas (1, 2, and 3) and frontal area 5 with signals from prefrontal area 9/46d ($n = 12$). Figure 5(b) shows the distribution of frequencies for all combinations of signals from somatosensory areas (1, 2, and 3) and frontal area 5 with

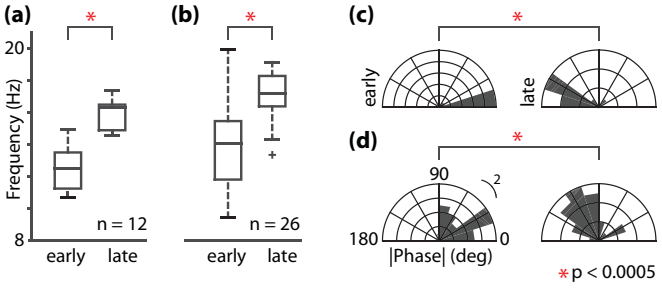

FIG. 5. Population data for signal pairs with prefrontal area 9/46d or prefrontal area 8L and the somatosensory areas (1, 2, and 3) and frontal area 5. (a) Synchronization frequencies for the early and late ITI for all signal pairs with prefrontal area 9/46d. (b) Synchronization frequencies for the early and late ITI for all signal pairs with prefrontal area 8L. (c) Relative phase angles for the early and late ITI for all signal pairs with prefrontal area 9/46d. (d) Relative phase angles for the early and late ITI for all signal pairs with prefrontal area 8L. Asterisk (*) indicates that medians are different at $p < 0.0005$.

signals from prefrontal area 8L ($n = 26$). In both instances, the median frequency is different between the early and late ITI (Wilcoxon signed rank test; paired, two sided; $p < 0.0005$). In general, the synchronization frequency increases between the early and late ITI. The relative phase data were split in the same manner. Figures 5(c) and 5(d) show the distribution of relative phase angles for signal pairs with prefrontal area 9/46d ($n = 12$), and prefrontal area 8L ($n = 26$), respectively. In both instances, the median relative phase angle is different between the early and late ITI (nonparametric multisample test for equal medians; $p < 0.0005$; see Ref. [18]). During the early ITI, relative phase values are concentrated near in phase, while during the late ITI the relative phase values consistently flip to near antiphase.

IV. DISCUSSION

In summary, we demonstrate that flips in the relative phase relationship between oscillatory narrow-band local field potential signals separated by several centimeters are accompanied by jumps in synchronization frequency. We find evidence for these phase-flip transitions on single trials (see Fig. 1), in trial averaged results (see Fig. 2), and at the population level (see Fig. 5). Specifically, we find that prefrontal areas 8L and 9/46d undergo a phase-flip transition with somatosensory areas 1, 2, and 3, and frontal area 5 during the ITI. There are also a variety of relative phase relationships and synchronization frequencies throughout the data set, indicating that these relationships are likely not dictated by a single common source (see Fig. 4).

What is the significance of these findings? Foremost is the demonstration that a characteristic property of coupled nonlinear oscillator systems with delays and other complex coupling schemes occurs in the brain between distant cortical areas. These findings help validate simplified models of neuronal coupling, and may help identify general principles of brain function. These findings are also significant to understanding the role of synchronization in the brain. Communication between neuronal groups is thought to be most effective when they are synchronized near 0° [19]. Recent studies—supported by laminar differences in cortical oscillations [20] and the laminar specificity of feedforward and feedback connections [21,22]—suggest that frequency specific channels may also provide a way to selectively communicate [23,24]. Based on these findings, changes in the relative phase and synchronization frequency between two neuronal groups would result in changes in the efficacy and/or directionality of interareal communication. The phase-flip transition may then act as a switch to modify the properties of interareal communication.

ACKNOWLEDGMENTS

This work was supported by the National Institute of Mental Health (Grant No. MH081162), the National Institute of Neurological Disorders and Stroke (Grant No. NS059312), and a McKnight Memory and Cognitive Disorders Award to C.M.G. We thank Baldwin Goodell for designing the microdrive recording system and Neuralynx (Neuralynx, Inc., Bozeman MT, USA) for providing the data acquisition system.

[1] H. G. Schuster and P. Wagner, Mutual entrainment of two limit cycle oscillators with time delayed coupling, Prog. Theor. Phys. **81**, 939 (1989).
[2] U. Ernst, K. Pawelzik, and T. Geisel, Synchronization Induced by Temporal Delays in Pulse-Coupled Oscillators, Phys. Rev. Lett. **74**, 1570 (1995).
[3] S. Kim, S. H. Park, and C. S. Ryu, Multistability in Coupled Oscillator Systems with Time Delay, Phys. Rev. Lett. **79**, 2911 (1997).
[4] M. Dhamala, V. K. Jirsa, and M. Ding, Enhancement of Neural Synchrony by Time Delay, Phys. Rev. Lett. **92**, 074104 (2004).
[5] A. Prasad, S. K. Dana, R. Karnatak, J. Kurths, B. Blasius, and R. Ramaswamy, Universal occurrence of the phase-flip bifurcation in time-delay coupled systems, Chaos **18**, 023111 (2008).
[6] A. Prasad, J. Kurths, S. K. Dana, and R. Ramaswamy, Phase-flip bifurcation induced by time delay, Phys. Rev. E **74**, 035204 (2006).
[7] B. M. Adhikari, A. Prasad, and M. Dhamala, Time-delay-induced phase-transition to synchrony in coupled bursting neurons, Chaos **21**, 023116 (2011).
[8] B. Akila and P. Muruganandam, Observation of phase-flip transition in delay-coupled Nishio-Inaba circuits, Eur. Phys. J. Spec. Top. **222**, 917 (2013).
[9] A. Takamatsu, T. Fujii, and I. Endo, Time Delay Effect in a Living Coupled Oscillator System with the Plasmodium of Physarum Polycephalum, Phys. Rev. Lett. **85**, 2026 (2000).
[10] J. M. Cruz, J. Escalona, P. Parmananda, R. Karnatak, A. Prasad, and R. Ramaswamy, Phase-flip transition in coupled electrochemical cells, Phys. Rev. E **81**, 046213 (2010).

[11] A. Sharma, M. D. Shrimali, A. Prasad, R. Ramaswamy, and U. Feudel, Phase-flip transition in relay-coupled nonlinear oscillators, Phys. Rev. E **84**, 016226 (2011).

[12] A. Sharma, M. D. Shrimali, and S. K. Dana, Phase-flip transition in nonlinear oscillators coupled by dynamic environment, Chaos **22**, 023147 (2012).

[13] N. Punetha, R. Karnatak, A. Prasad, J. Kurths, and R. Ramaswamy, Frequency discontinuity and amplitude death with time-delay asymmetry, Phys. Rev. E **85**, 046204 (2012).

[14] N. M. Dotson, R. F. Salazar, and C. M. Gray, Frontoparietal correlation dynamics reveal interplay between integration and segregation during visual working memory, J. Neurosci. **34**, 13600 (2014).

[15] N. M. Dotson, B. Goodell, R. F. Salazar, S. J. Hoffman, and C. M. Gray, Methods, caveats and the future of large-scale microelectrode recordings in the non-human primate, Front. Syst. Neurosci. **9**, 149 (2015).

[16] R. F. Salazar, N. M. Dotson, S. L. Bressler, and C. M. Gray, Content-specific fronto-parietal synchronization during visual working memory, Science **338**, 1097 (2012).

[17] P. König, A method for the quantification of synchrony and oscillatory properties of neuronal activity, J. Neurosci. Methods **54**, 31 (1994).

[18] N. I. Fisher, *Statistical Analysis of Circular Data* (Cambridge University Press, Cambridge, UK, 1995).

[19] P. Fries, A mechanism for cognitive dynamics: Neuronal communication through neuronal coherence, Trends Cognit. Sci. **9**, 474 (2005).

[20] E. A. Buffalo, P. Fries, R. Landman, T. J. Buschman, and R. Desimone, Laminar differences in gamma and alpha coherence in the ventral stream, Proc. Natl. Acad. Sci. USA **108**, 11262 (2011).

[21] N. T. Markov, M. Ercsey-Ravasz, D. C. Van Essen, K. Toroczkai, Z. Knoblauch, and H. Kennedy, Cortical high-density counter-stream architectures, Science **342**, 1238406 (2013).

[22] N. T. Markov, J. Vezoli, P. Chameau, A. Falchier, R. Quilodran, C. Huissoud, and P. Barone, Anatomy of hierarchy: Feedforward and feedback pathways in macaque visual cortex, J. Comp. Neurol. **522**, 225 (2014).

[23] T. Van Kerkoerle, M. W. Self, B. Dagnino, M. A. Gariel-Mathis, J. Poort, C. Van Der Togt, and P. R. Roelfsema, Alpha and gamma oscillations characterize feedback and feedforward processing in monkey visual cortex, Proc. Natl. Acad. Sci. USA **111**, 14332 (2014).

[24] A. M. Bastos, J. Vezoli, C. A. Bosman, J. M. Schoffelen, R. Oostenveld, J. R. Dowdall, and P. Fries, Visual areas exert feedforward and feedback influences through distinct frequency channels, Neuron **85**, 390 (2015).